Journal of Multidisciplinary Engineering Science and Technology (JMEST)
ISSN: 2458-9403
Vol. 4 Issue 10, October - 2017

Assessing of the suitability of using a diamond detector made based on graphitized electrodes under Nd:YAG laser irradiation as a semiconductor microdosimeter

F. Payervand[a], G. Raisali[a], S. Saramad[c*], F. Hajiesmaeilbaigi[b]

a Radiation Applications Research School, Nuclear Science and Technology Research Institute, AEOI, P.O.Box: 11365-3486, Tehran, Iran
b Photonics and Quantum Technologies Research School, Nuclear Science and Technology Research Institute, AEOI, P.O.Box: 11365-8486, Tehran, Iran
c Energy Engineering and Physics Faculty, Amirkabir University of Technology, P.O.Box: 15875-4413, Tehran, Iran
* Corresponding author: Shahyar Saramad, Energy Engineering and Physics Faculty, Amirkabir University of Technology, P.O.Box: 15875-4413, Tehran, Iran.
E-mail: ssaramad@aut.ac.ir

***Abstract*—Semiconductor microdosimeters are appropriate candidate for dose equivalent measurement of unknown and complex radiation fields such as fields of hadron-therapy and space. Among them the diamond microdosimeters are superior because of the favorable properties of the detector-grade diamond. The main goal of this work is feasibility study of using a Nd:YAG laser beam to create graphitized electrodes and hence, a sensitive volume (SV) in diamond for microdosimetry applications in radiation protection domains. For this purpose, a combination of the finite element method and Geant4 Monte Carlo toolkit is used. The results show that for the SV of an undoped diamond detector created by a Gaussian profile laser beam with radius of 5 µm, pulse duration of 20 ns, focusing depth of 6 µm and fluence of 4.98×1016 mW/m2 under 25 V bias and for charge collection efficiencies higher than 20% and charge collection times less than 50 ns, the estimated mean chord length is relatively large, aboute 50 µm. It is observed that the linear stopping power of the protons with energies higher than 5 MeV can be estimated within 20% of deviation using the microdosimeter response. The dose equivalent response ratio of the SV to the response of a spherical SV with 1 µm diameter is calculated for mono-energetic protons from 1 to 105 MeV using the lineal energy based quality factor recommended by ICRU and ICRP joint grope. Obtained results reveal that the dose equivalent response of the SV is calculated lower than that of the spherical SV with 1 µm diameter by a factor of 3. Thus, the response of the microdosimeter should be used by applying a corrected factor to compensate the effect of larger sensitive volume of the microdosimeter.**

Keywords—Laser induced diamond graphitization; Microdosimetry; dose equivalent; Monte Carlo simulation; Geant4 toolkit

I. INTRODUCTION

In ion radiation fields such as fields of space and hadron therapy, the radiation quality varies consistently as the particles slow down and/or produce secondary particles. In this case, the radiation field is unknown and complex, for which the type and the energy spectra for assessing the local radiation quality with small detectors is not possible [1]. In this case, the radiation quality can be specified in terms of lineal energy spectra which is the quotient of the energy imparted to matter in a volume of interest in a single event by the mean chord length of that volume [2]. Microdosimeters are devices that can be used for these applications. Works of Rossi and coworkers in 1950 [3] led to develop the first microdosimeter device, a low-pressure proportional counter which commonly called the Rossi counter. The standard measurement device in microdosimetry is a Rossi counter that is tissue equivalent and called the tissue equivalent proportional counter (TEPC) [1, 4, 5]. TEPC suffers from weaknesses such as the low spatial resolution, the requirement to high electrical power and the dependency of the response to pressure and temperature. To overcome these weaknesses, using semiconductor microdosimeters is a good option. Silicon microdosimeters have been studied since 1980 by Dicello and their results have been compared with spherical TEPCs [6]. Some disadvantages of these microdosimeters, such as the absence of the tissue equivalency, low sensitivity and low resistance to radiation, lead to the development of more suitable microdosimeters for this purpose. Diamond is very promising in this regard. Microdosimeters based on the

so-called detector-grade CVD diamond materials have been proposed for radiobiology, radiotherapy dosimetry and space radioprotection applications over the last few years [5, 7] because of their favorable properties such as more tissue equivalency, higher radiation hardness, lower temperature dependency, less dark current, noise and sensitivity to visible light [8, 9]. In order to use CVD diamond as a radiation detector, two electrodes are needed for applying the potential differences to collect the charge carriers. One of the methods for creating electrodes for diamond is making the graphitized electrodes by converting diamond to graphite as a conductive layer. Burgemeister [10] and Geis [11] were among the first that individually have provided a method to make a strong electrical contact in the regions with an increased conductivity created under laser irradiation. Alemanno recently used a similar method to create graphitized electrodes in a diamond detector [12]. He has measured the electrical resistivity of the graphitized electrodes and has shown that by this method an ohmic contact can be established. De Feudis and coworkers also, have characterized the integrated graphitic contacts on a diamond produced by means of laser irradiation, [13]. One of the advantages of this method is that the electrodes are created in a single step at room temperature. The purpose of this work is the feasibility study of using the sensitive volume (SV) provided by applying voltage to the graphitized electrodes created under irradiation of diamond by Nd:YAG (λ=1064 nm) laser beam, for microdosimetry and radiation protection applications. In this work, by using the finite element method, the parameters affecting sensitive volume determination have been estimated. Then, the mean chord length of the SV has been determined by Monte Carlo simulation using Geant4 toolkit. The calculation methodology and the Geant4 application program developed in this work has been verified by estimating the LET values of the mono-energetic protons and comparing them with the linear stopping powers reported by NIST for water [14]. The dose equivalent response of the studied SV has been estimated for mono energetic protons from 1 to 105 MeV and compared with the dose equivalent response of a spherical SV with 1 μm diameter from ICRU tissue substance [15]. In ion radiation fields such as fields of space and hadron therapy, the radiation quality varies consistently as the particles slow down and/or produce secondary particles. In this case, the radiation field is unknown and complex, for which the type and the energy spectra for assessing the local radiation quality with small detectors is not possible [1]. In this case, the radiation quality can be specified in terms of lineal energy spectra which is the quotient of the energy imparted to matter in a volume of interest in a single event by the mean chord length of that volume [2]. Microdosimeters are devices that can be used for these applications.

Works of Rossi and coworkers in 1950 [3] led to develop the first microdosimeter device, a low-pressure proportional counter which commonly called the Rossi counter. The standard measurement device in microdosimetry is a Rossi counter that is tissue equivalent and called the tissue equivalent proportional counter (TEPC) [1, 4, 5]. TEPC suffers from weaknesses such as the low spatial resolution, the requirement to high electrical power and the dependency of the response to pressure and temperature. To overcome these weaknesses, using semiconductor microdosimeters is a good option. Silicon microdosimeters have been studied since 1980 by Dicello and their results have been compared with spherical TEPCs [6]. Some disadvantages of these microdosimeters, such as the absence of the tissue equivalency, low sensitivity and low resistance to radiation, lead to the development of more suitable microdosimeters for this purpose. Diamond is very promising in this regard. Microdosimeters based on the so-called detector-grade CVD diamond materials have been proposed for radiobiology, radiotherapy dosimetry and space radioprotection applications over the last few years [5, 7] because of their favorable properties such as more tissue equivalency, higher radiation hardness, lower temperature dependency, less dark current, noise and sensitivity to visible light [8, 9]. In order to use CVD diamond as a radiation detector, two electrodes are needed for applying the potential differences to collect the charge carriers. One of the methods for creating electrodes for diamond is making the graphitized electrodes by converting diamond to graphite as a conductive layer. Burgemeister [10] and Geis [11] were among the first that individually have provided a method to make a strong electrical contact in the regions with an increased conductivity created under laser irradiation. Alemanno recently used a similar method to create graphitized electrodes in a diamond detector [12]. He has measured the electrical resistivity of the graphitized electrodes and has shown that by this method an ohmic contact can be established. De Feudis and coworkers also, have characterized the integrated graphitic contacts on a diamond produced by means of laser irradiation, [13]. One of the advantages of this method is that the electrodes are created in a single step at room temperature.

The purpose of this work is the feasibility study of using the sensitive volume (SV) provided by applying voltage to the graphitized electrodes created under irradiation of diamond by Nd:YAG (λ=1064 nm) laser beam, for microdosimetry and radiation protection applications. In this work, by using the finite element method, the parameters affecting sensitive volume determination have been estimated. Then, the mean chord length of the SV has been determined by Monte Carlo simulation using Geant4 toolkit. The calculation methodology and the Geant4 application program developed in this work has been verified by estimating the LET values of the mono-energetic protons and comparing them with the linear stopping powers reported by NIST for water [14]. The dose equivalent response of the studied SV has been estimated for mono energetic protons from 1 to 105 MeV and compared with the dose equivalent response of a

spherical SV with 1 μm diameter from ICRU tissue substance [15].

II. Materials and Methods

Graphitized Electrodes

For determination of the graphitized region in the laser irradiated diamond the temperature distribution inside the sample should be determined. In this section, the methodology and the governing equations are explained. The laser beam specifications, material properties, the geometry of the produced dosimeter and the boundary conditions are also explained.

Heat conduction equation and volumetric heating term

Laser irradiation of a matter causes a localized heating which changes the temperature inside the irradiated sample. By clarifying the amount of energy accumulated in the matter as enthalpy and taking into account the contribution of external laser as an external energy source $S(x,y,z,t)$, heat diffusion equation in three dimensions can be explained by [16]:

$$\frac{dT}{dt} = \frac{k}{\rho c_P}\nabla^2 T + \frac{1}{\rho c_P}(\nabla k.\nabla T) + \frac{S(x,y,z,t)}{\rho c_P} \quad (1)$$

Where x, y and z are the Cartesian coordinates, T is the temperature, k is the thermal conductivity, c_P is the specific heat at constant pressure and ρ is the matter density. The volumetric heating term S(x,y,z,t), regardless of phase changes or chemical reactions at any point in depth z at time t is [17]:

$$S(x,y,z,t) = \alpha(1 - R)I_0 exp(-\alpha z)\exp\left[-\frac{x^2+y^2}{\left(\frac{r}{\sqrt{\ln 2}}\right)^2}\right] exp\left[-\left(\frac{t}{\frac{\tau}{2\sqrt{\ln 2}}}\right)^2\right] - \frac{L_m \rho}{\tau} \quad (2)$$

where α is the absorption coefficient, R is the reflectivity, I_0 is the incident laser beam intensity, r is the radius of the laser beam at half maximum, τ is the pulse duration, L_m is the latent heat of fusion. The solution of Eq. (1) generally requires numerical methods. In this work the finite element method was used to solve Eq. (1) with $S(x,y,z,t)$ given by Eq. (2).

Laser beam specifications, material properties and applied geometry

As shown in Fig. 1, for reducing the simulation time, the geometry of the diamond sample was considered as a rectangle with dimensions of 20 μm × 40 μm which was irradiated by Nd:YAG laser beam. The specifications of the laser beam are presented in Table 1. The laser beam energy was selected in such a way that the temperature of the irradiated region rises to higher than the graphitization threshold temperature which starts the graphitization process. Moreover, it was assumed that a single shot of laser is sufficient for the graphitization process.

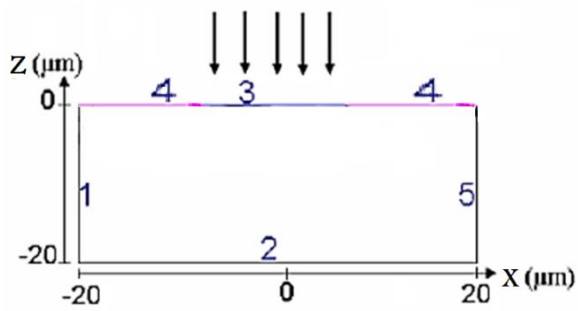

Fig. 1. Geometry of diamond used in the simulation. The diamond sample was irradiated by the laser beam along the Z axis in the boundary 3.

Table 1. Specification of the simulated laser beam, thermo-physical and optical properties of diamond and graphite

Parameter	Quantity	Dimension
Laser Pulse Profile	Gaussian	-
Laser Pulse Duration	20	ns
Laser Wave Length	1.064	μm
Laser Beam Radius in Focusing Point	5.0	μm
Absorption Coefficient of Graphite [18]	2.88×10^7	1/m
Absorption Coefficient of Diamond (@1073 K) [19]	79.0	1/m
Latent Heat of Fusion of Graphite [20]	8750	J/g
Density of Diamond (@ 300 K) [21]	3515	kg/m^3
Density of Graphite [20]	2260	kg/m^3
Thermal Conductivity of Diamond (@ 300 K) [21]	2275	W/mK
Thermal Conductivity of Graphite[20]	120	W/mK
Specific Heat Capacity of Diamond (@ 300 K) [21]	477	J/kgK
Specific Heat Capacity of Graphite [20]	1762	J/kgK

Graphitization and boundary conditions

It can be assumed that the graphitization is a pyrolitic process which can be considered as a result of rising the temperature [22]. In the literature the graphitization threshold temperature of diamond was reported in the range of 1000 to 2000 K [11, 23, 24]. In this work, the threshold temperature of the graphitization of diamond was chosen to be 1073 K which is reported more often [22]. In this way, the region of the diamond under laser irradiation becomes graphitized when its temperature rises to higher than 1073 K.

Heat exchange is carried by convection and radiation in surfaces of material and can be considered by applying the suitable boundary conditions [17]. For the boundary conditions, it was assumed that the heat on the boundary 3 in Fig. 1 can be transferred to the environment by radiation and convection, while, the other boundaries were considered thermal insulation.

2.2. Sensitive volume of the microdosimeter

In order to determine the lineal energy spectrum of a microdosimeter, its SV should have been specified. The most important parameters that affect the SV of the microdosimeter are the dimensions of graphite electrodes, the quality of created graphite, the purity

and properties of diamond substrate and the voltage applied to the electrodes. In this work, for an undoped diamond substrate with properties mentioned in Table 2, the optimum voltage for the microdosimeter response and the method of determining the SV and mean chord length of the SV of the microdosimeter are presented.

Tabal 2. Material properties used in the simulation

Parameter	Quantity	Dimension
Diamond Band Gap [25]	5.47	V
Diamond Work Function [26]	1.29	V
Graphite Work Function [27]	4.83	V
Diamond Electron Affinity	-0.4	eV
Electron Mobility for Diamond [25]	0.45	m^2/Vs
Hole Mobility for Diamond [25]	0.38	m^2/Vs

Optimum voltage for the microdosimeter response

In many applications, for using a semiconductor as a radiation detector, an ohmic contact is needed [11]. One of the indicators of the goodness of an ohmic contact is specific contact resistivity ρ_c, that is defined as the reverse of the derivative of the current density J to the voltage V at zero bias voltage [28]:

$$\rho_c = \left(\frac{\partial J}{\partial V}\right)^{-1}\Big|_{V=0}$$

(3)

For a good ohmic contact, ρ_c should be as small as possible and negligible compared to bulk resistivity. The optimal voltage range is where the contact resistivity of the connection structure is constant.

2.2.2. Method for defining the sensitive volume

To specify the sensitive volume of a semiconductor detector, ratio of the collected charge to the generated charge (i.e. charge collection efficiency (CCE)), as well as, charge collection time must be determined as a function of the position of the generated charge [5]:

$$CCE(x,y,z) = \frac{Q_{coll}(x,y,z)}{Q_{gen}(x,y,z)}$$

(4)

where $Q_{coll}(x,y,z)$ and $Q_{gen}(x,y,z)$ are the collected and the generated charge in (x,y,z) point, respectively.

In this work, for determining the amount of the collected charge on the respective electrodes, the induced charge caused by the drift of carriers created in different points inside the diamond microdosimeter was estimated by Schockley-Ramo theorem [29]. For this, finite element method was used. The spatial distribution of the charge collection efficiency due to each point of considered creation charge point was determined by Eq. (4). The spatial distribution of the charge collection time (traveling time of the charge carriers between the considered point of creation and respective electrodes) was specified, also. The SV of the detector is considered in a region where the charge collection efficiency is more than 0.333 of the central electrode region and also the charge collection time is less than 50 ns [30]. The charge collection time criterion of 50 ns has been chosen as a nominal collection time that can be handled by a common electronic system.

2.2.3. Mean chord length determination

Determination of mean chord length of the SV is essential for specifying the lineal energy, y. The lineal energy is a measure of the stochastic energy deposited along a given chord length of the sensitive volume of the microdosimeter [2]:

$$y = \frac{\epsilon}{\bar{l}}$$

(5)

where ϵ is the energy imparted in the SV and $\bar{l}$ is the mean chord length of the SV. The mean chord length of irregular geometric shapes can be calculated using their chord length distribution function "$f(l)$" [5]:

$$\bar{l} = \int_0^\infty l f(l)\, dl$$

(6)

In this work, the chord length distribution function of the intended sensitive volume was obtained using developed Geant4 application by defining Geantino as the incident radiation. Geantino is a virtual particle which is used for simulation purposes and merely undertakes transportation processes without doing any interaction with materials.

Microdosimeter response

Monte Carlo simulation

In this work, a Geant4 application was developed and used for modeling the electromagnetic and hadronic interactions of an incident proton or alpha particle with SV of the diamond microdosimeter. The incident particles were directed from vacuum towards the SV. An isotropic spherical particle source with 1 m radius with cosine-law angular emission was considered around SV. Since the particle generator surface is enough far from the SV, the distribution can be considered isotropic [31]. In order to reduce the simulation time, the primary particle emission angle was limited to $0 \leq \theta < arctan(l/10^6)$. Where l is the largest length of the SV in μm.

As QGSP_BIC_HP physics list of Geant4 toolkit is verified with experimental results in a proton radiation field [32], it was chosen for modeling the hadronic physics processes. In order to consider all the electromagnetic interactions of particles down to 250 eV, the Low Energy Physics Package based on Livermore data libraries [33] was used. The primary and secondary particles were tracked in the simulation with cutoff range of 0.01 μm, and the output of the simulation was the energy deposition of the particles and track length per step in the SVs. The number of incident particles for each case was selected enough large to achieve a relative statistical uncertainty of less than 0.5% for the total energy deposition in the SV.

Microdosimeter response calculation

To determine the lineal energy distribution for a given radiation and the SV size, the energy imparted to the SV in each ionization event is calculated and is divided by the mean chord length of the SV. By setting the logarithmic bins of the lineal energy, and by

scoring the frequency of events in each bin, the lineal energy distribution " $f(y)$ " is determined. After determining the lineal energy distributions, the dose equivalent response *H* is estimated by Eq. (7) [34]:

$$H = D \int Q(y) \frac{y f(y)}{\bar{y}_F} dy \quad (7)$$

where y is the lineal energy in keV/μm , $D = \frac{n \bar{l}_F \bar{y}_F}{m_{SV}}$ is the absorbed dose, $Q(y)$ is the quality factor, $\bar{l}_F$ is the mean chord length of the SV, m_{SV} is the mass of SV, *n* is the number of events and $\bar{y}_F$ is the frequency-average of lineal energy. For a sphere with 1 μm diameter, $Q(y)$ is obtained from Eq. (8) [35]:

$$Q(y) = 0.3y \left[1 + \left(\frac{y}{137}\right)^5\right]^{-0.4} \quad (8)$$

III. Results and Discussion

The graphitized electrodes study

By selecting the laser beam energy in such a way to start the graphitization process in laser beam focusing point, it has been observed that some part of the laser irradiated diamond is evaporated and some region is converted to graphite. Depth and diameter of the graphitization and evaporation regions formed under irradiation of the focused laser beam in different depths in diamond is presented in Fig. 2. As can be seen, by increasing the depth of the focused laser beam, the depth of the graphitization region is also increased, but the graphitization and evaporation diameter and evaporation depth are decreased. This decrease is because the energy transferred to the surface of the diamond sample has decreased.

Fig. 3 denotes that the threshold fluence which is needed to start the laser graphitization process when the focusing point of the laser beam is in the surface of the diamond sample is about 6.5×10^9 W/cm^2 (6.5×10^{16} mW/m^2). This is in agreement with the fluence required for starting the process of graphitization of the diamond with a Nd:YAP (λ=1078 nm) laser beam that is measured experimentally and reported by Kononenko et al [36]. Kononenko and coworkers with Nd:YAP laser beam with spatial profile of nearly Gaussian and pulse width of 9 ns have observed that a crater can be created by a single pulse shot at 4.8×10^9 W/cm^2. Moreover, Fig. 3 shows that by increasing the depth of focus of the laser beam with duration of 20 ns, the fluence needed to start the graphitization process is decreased and reached to a broadened minimum. This behavior is predictable, because by increasing the depth of the focus of the laser beam, the energy transferred to the surface of the diamond sample is decreased as well as the energy loss due to radiation and convection is also decreased.

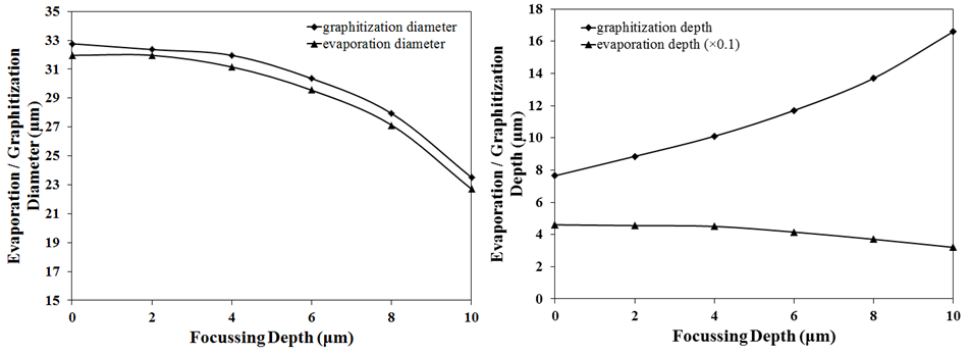

Fig. 2. **Right**: depth of evaporation and graphitization and **Left**: diameter of evaporation and graphitization regions formed under irradiation by the laser beam with pulse duration of 20 ns and different focused depths.

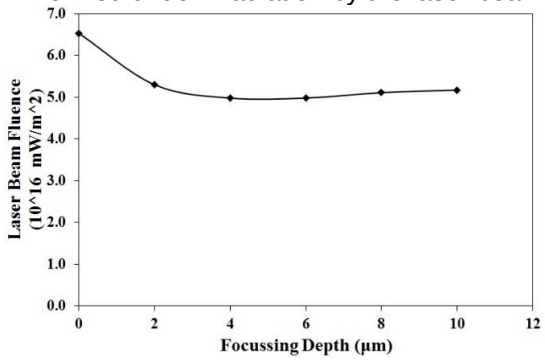

Fig. 3. Laser beam fluence needed to start the graphitization process according to the depth of focus of the laser beam with pulse duration of 20 ns.

According to Fig. 3, the threshold energy which is needed to start the laser graphitization process is related to the depth of focusing the laser beam in diamond, therefore, since less laser beam energy, less evaporation of diamond and low depth and diameter of the graphitized region of diamond is desirable, the depth of focusing of the laser beam was chosen as 6 μm. In this case, the graphitization boundary profile created by 4.98×10^{16} mW/m^2 laser beam fluence with a Gaussian energy profile has a bell shape that can be approximated by a Gaussian distribution with FWHM of about 33 μm to simplify the simulation of the charge collection process and specifying the SV of the microdosimeter. In this way, with irradiation of a diamond sample by sufficiently intense and energetic laser beam, a graphitized region can be created in the background and can be used as an electrical electrode. The laser pulse duration and frequency used in this method should be proportional to the speed of the sample movement in such a way that the graphitized regions of the diamond are Inter-connected. The process has the disadvantage of heating the bed up to a high temperature, and heat may be directed to regions

outside the optimal area, and adjacent areas may also be graphitized.

In this work, assuming that the diamond sample has been properly moved under the laser beam, microdosimeter cells have be considered in the diamond sample somehow that each cell (SV) has a central and a peripheral graphite electrode. Both central and the peripheral electrodes are assumed that have Gaussian cross-sections. The central electrode is positioned in the middle of the microdosimeter cell is surrounded by the peripheral cylindrical graphite electrode (Fig. 4). The diameter of central electrode, its depth and the inner and outer radius of peripheral electrode were considered 40, 12, 40 and 80 μm, respectively.

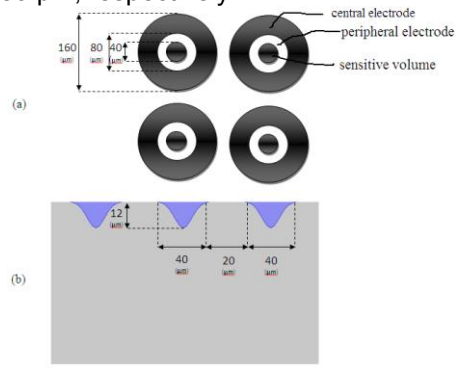

Fig. 4. Schematic views of the diamond microdosimeter: (a) top view, (b) side view.

The sensitive volume study

Optimum voltage of operating undoped diamond

In this section the results of the optimum applied voltage for an undoped diamond with specifications given in Table 2 are presented. Fig. 5 shows the variations of the specific contact resistivity of the diamond-graphite structure at 300 K. According to this result, the specific contact resistivity of the diamond-graphite structure is not symmetric for positive and negative voltages. This figure shows that for the voltages of 20 to 40 V and -20 to -40 V, the specific contact resistivity of the diamond-graphite structure at 300 K can approximately considered constant. The specific contact resistivity of the diamond-graphite structure at zero voltage can be derived from the data depicted in Fig. 5. The contact resistance can be calculated by taking into account the length and the cross sectional area of the diamond-graphite structure. The calculated contact resistance for the intended diamond-graphite structure is $(1.57\pm0.02)\times10^{6}$ Ω which is negligible compared to the bulk resistance of the diamond with bulk resistivity of about 10^{18} Ωm [37, 38] and bulk resistance of about 10^{22} Ω for the diamond sample with dimensions of 40 μm × 40 μm × 20 μm.

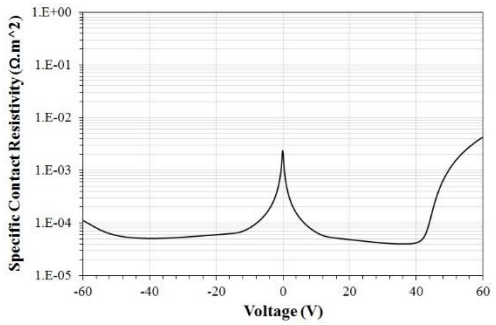

Fig. 5. Specific contact resistivity of the diamond-graphite structure at 300 K.

Fig. 6 indicates the variations of specific contact resistivity of diamond-graphite structure with temperature. This figure shows that by increasing the temperature, the specific contact resistivity is decreased. Since the specific contact resistivity of the diamond-graphite structure is constant roughly in the voltage ranges of 20 to 30 and -20 to -30 volts, the bias voltage of 25 V is suitable for more stable operation of the detector in case of applied voltage changes.

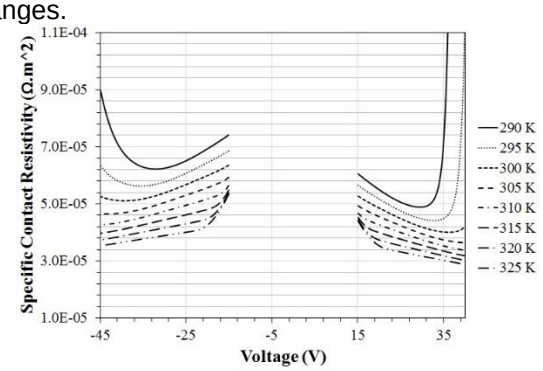

Fig. 6. Variations of the specific contact resistivity of the diamond-graphite structure.

Sensitive volume size and shape

In this section, the shape of SV for the diamond-graphite structure with Gaussian graphitized electrodes, for 25 V applied voltage between the electrodes is estimated. At this voltage the diamond-graphite contact is approximately ohmic, according to results presented in Section 3.2.1.

In Fig. 7, the boundary of the regions for which the charge collection efficiency is more than 0.333 of the central electrode region (the regions with charge collection efficiencies more than 20%) and also the charge collection times are less than 50 ns, are considered as the SV of the detector. It should be mentioned that the charge collection efficiency of each graphitized electrode is maximum near the central electrode and decreases by going in depth and side directions. By this method, there is not a clear border to find out the SV. Thus, similar to all solid state detectors the diamond microdosimeter also suffers from the precise determination of the sensitive volume. On the other hand in order to calculate the lineal energy spectrum of the microdosimeter, the SV must have a definite boarder. To overcome this deficiency the charge collection time is considered as

an auxiliary parameter to define the microdosimeter SV precisely.

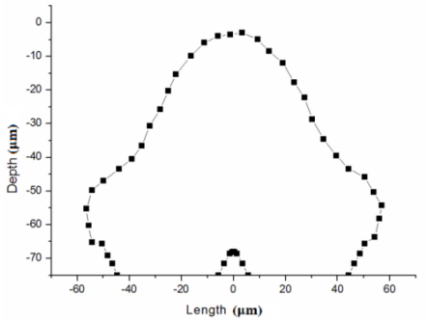

Fig. 7. Boundary regions with charge collection efficiencies greater than 20% and charge collection time of less than 50 ns in the microdosimeter.

Mean chord length study

Considering the shape and size of the SV, the geometry of the sensitive volume of the microdosimeter was divided to 15 co-axial cylindrical slabs with different dimensions (Fig. 8) stacked on each other to form the whole volume. Fig. 9 shows the distribution of the chord length of the SV, "*f(l)*", of the detector. Based on the chord length distribution function, the mean chord length of the microdosimeter is calculated as around 50 µm (according to Eq. (6)).

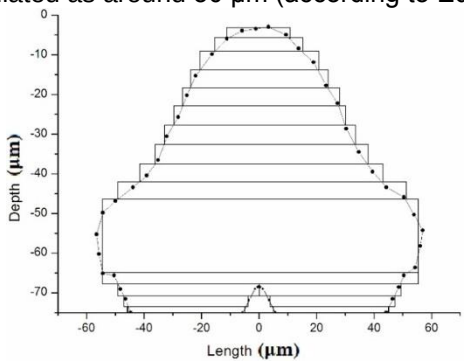

Fig. 8. The layout and dimensions of the sensitive volume in the diamond microdosimeter formed from different co-axial slab cylinders.

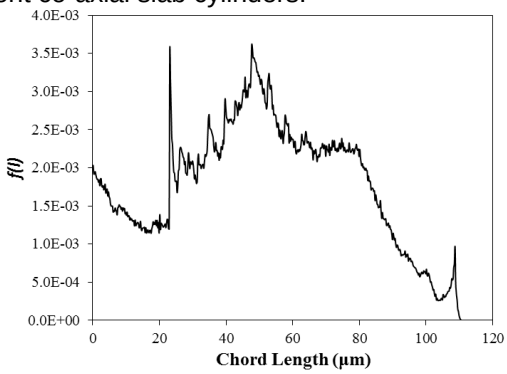

Fig. 9. Chord length distribution function of the diamond sensitive volume.

The microdosimeter response

Estimating the linear energy transfer by Microdosimeter response

Fig. 10 shows the ratio of the frequency-averaged lineal energy of mono-energetic protons determined by the microdosimeter response to the linear stopping power reported by NIST for water [14]. As can be seen, the linear stopping power of the protons with energies greater than 5 MeV can be estimated using the studied microdosimeter with a relative error less than 20%. Moreover, the figure shows that the ratio of the frequency-averaged lineal energy decreases severely in the energies less than 5 MeV. The severe decrease in the ratio of the frequency-averaged lineal energy in the energies can be related to the dimensions of the microdosimeter sensitive volume. Since, most protons with these energies are stopped within such SVs without crossing the boundaries, the amount of their lineal energies, and hence the frequency-averaged lineal energies underestimate the linear stopping power. Nevertheless, since the linear stopping power of the protons with energies greater than 5 MeV, are estimated with a relative error of less than 20%, the absorbed dose is expected to be determined within an acceptable uncertainty for radiation protection applications.

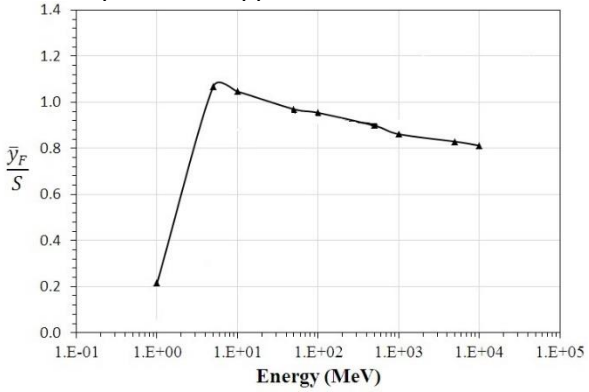

Fig. 10. The ratio of the calculated frequency-averaged lineal energy "$\bar{y}_F$" of the diamond microdosimeter to the linear stopping power "S" for various proton energies. The linear stopping powers for water are from NIST [21].

Dose equivalent response of the microdosimeter

The ratio of the dose equivalent response of the microdosimeter to the response of a spherical SV with 1 µm diameter for 6 selected energetic protons is given in Fig. 11. As shown in the figure, for energies greater than 10 MeV by increasing the proton energy, the ratio of the dose equivalent responses has a decreasing behavior, which is about three times less than the response of a spherical SV with 1 µm diameter for high energies. Because, by increasing the energy of incident particle, for energies higher than 10 MeV, the energy loss straggling becomes more important and greater amount of energy can escape from the SV [39], so the microdosimetric spectra shifts to lower lineal energies in such a way that the frequency-average of the lineal energy and the absorbed dose approximately remain unchanged [40]. By shifting the microdosimetric spectra to lower lineal energies, the quality factor calculated by Eq. (8) is decreased. Hence, the dose equivalent response of the microdosimeter is also decreased. Since the variation of the dose equivalent response is dominant by the quality factor, the quality factor calculated by

Eq. (8) which is valid only for a spherical SV with diameter of 1 μm, is not suitable for the proposed microdosimeter with a large SV.

Alternatively, for energies less than 10 MeV, by decreasing the energy, the ratio of dose equivalent response also decreases. The reason is that by decreasing the energy the range of the incident particles decreases and most of them become stopper. Then, their lineal energies are estimated less than the actual value which makes the absorbed dose to be underestimated.

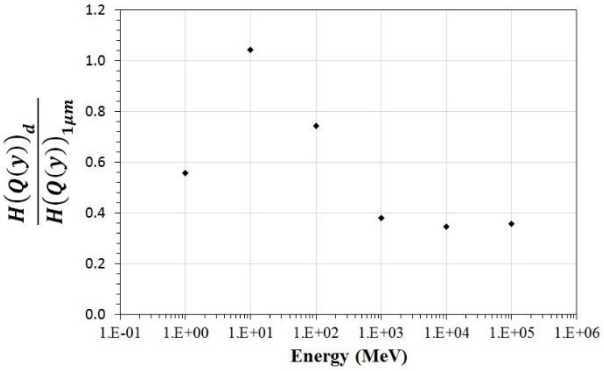

Figure 11. Ratio of dose equivalent response of the microdosimeter to the response of the spherical SV with 1 μm diameter using $Q(y)$.

IV. Conclusion

In the present work, by using the finite element method and Monte Carlo simulation it was found that the required laser beam fluence to start the graphitization process in the diamond depends on the depth of the focused laser beam. The required fluence for graphitization decreases by increasing the depth of the focused laser beam. The simulation results also showed that by increasing the depth of the focused laser beam the depth of the graphitization region is increased, while, the diameter of the graphitization region and the depth and the diameter of the evaporation regions are decreased.

Moreover, the study of the SV shape reveals that the detector, similar to other solid state detectors suffers from SV uncertainty. Thus, for more precise determination of the SV of the microdosimeter, the charge collection time of 50 ns was also chosen as an auxiliary decision parameter.

The microdosimeter response study indicates that the linear stopping power of the protons with energies greater than 5 MeV, can be estimated with a relative error less of than 20%. By studying the ratio of the dose equivalent response of the microdosimeter to the dose equivalent response of a spherical SV with 1 μm diameter, it was observed that the dose equivalent response of this microdosemeter with large SV be up to three times less than that of the spherical SV with 1 μm diameter for mono energetic protons. Therefore, the technique employed to creation of the diamond graphitized electrodes must be corrected through using a femtosecond laser beam or a correction factor should be applied to the Q(y) to get better estimate of the dose equivalent response of the diamond microdosimeter under study.

V. References

[1] Verona C, Magrin G, Solevi P, Grilj V, Jakšić M, Mayer R, et al. Spectroscopic properties and radiation damage investigation of a diamond based Schottky diode for ion-beam therapy microdosimetry. Journal of Applied Physics. 2015;118(18):184503.

[2] Rossi BHH, Zaider M. Microdosimetry and its Applications: Springer; 1996.

[3] Rossi HH, Rosenzweig W. A device for the measurement of dose as a function of specific ionization. Radiology. 1955;64(3):404-11.

[4] Davis JA, Guatelli S, Petasecca M, Lerch ML, Reinhard MI, Zaider M, et al. Tissue equivalence study of a novel diamond-based microdosimeter for galactic cosmic rays and solar particle events. IEEE Transactions on Nuclear Science. 2014;61(4):1544-51.

[5] Bradley PD. The development of a novel silicon microdosimeter for high LET radiation therapy: University of Wollongong; 2000.

[6] Dicello J, Amols H, Zaider M, Tripard G. A comparison of microdosimetric measurements with spherical proportional counters and solid-state detectors. Radiation Research. 1980;82(3):441-53.

[7] Wroe AJ. Developments in microdosimetry and nanodosimetry for space and therapeutic applications: University of Wollongong; 2007.

[8] Davis JA, Ganesan K, Alves AD, Guatelli S, Petasecca M, Livingstone J, et al. Characterization of a novel diamond-based microdosimeter prototype for radioprotection applications in space environments. IEEE Transactions on Nuclear Science. 2012;59(6):3110-6.

[9] Rollet S, Angelone M, Magrin G, Marinelli M, Milani E, Pillon M, et al. A novel microdosimeter based upon artificial single crystal diamond. IEEE Transactions on Nuclear Science. 2012;59(5):2409-15.

[10] Burgemeister EA, inventor; U.S. Patent No. 4,511,783, assignee. Method for making electrical contacts to diamond by means of a laser, and diamond provided with contacts according to this optical method patent 4511783. 1985.

[11] Geis MW, Rothschild M, Ehrlich DJ, inventors; U.S. Patent No. 5,002,899, assignee. Electrical contacts on diamond patent 5002899. 1991.

[12] E. Alemanno AC, M. Catalano, G. Chiodini, G. Fiore, M. Martino, R. Perrino, C. Pinto, S. Spagnolo. Diamond detector with laser made graphitic electrodes. Italy: Istituto Nazionale di Fisica Nucleare, 2011.

[13] De Feudis M, Caricato A, Martino M, Alemanno E, Ossi P, Maruccio G, et al., editors. Realization and characterization of graphitic contacts

on diamond by means of laser. 4th Workshop-Plasmi, Sorgenti, Biofisica ed Applicazioni; 2015.

[14] Berger MJ, Coursey J, Zucker M, Chang J. Stopping-power and range tables for electrons, protons, and helium ions: NIST Physics Laboratory; 1998.

[15] Tissue Substitutes in Radiation Dosimetry and Measurement. International Commission on Radiation Units and Measurements., 1989 0579-5435 Contract No.: no. 44.

[16] Sharma MK. Optimization of laser induced forward transfer by finite element modeling: Royal Institute of Technology; 2013.

[17] Matthew S. Brown CBA. Fundamentals of Laser-Material Interaction and Application to Multiscale Surface Modification. Laser Precision Microfabrication. Verlag Berlin Heidelberg Springer; 2010.

[18] M. Khaleeq-ur- Rahman MSR, Khurram Siraj, Shazia Shahid, M. S. Anwar, and Hafsa Faiz. Theoretical and Experimental Comparison of Splashing in Different Materials. 31st EPS Conference on Plasma Phys London2004.

[19] Z. Remes MN. Local variations and temperature-dependence of optical absorption coefficient in natural IIa type, CVD diamond and ZnSe optical windows. 11 th European Conference on Diamond, Diamond-like Materials, Carbon Nanotubes, Nitrides and Silicon carbide; 2000; Porto2000.

[20] entegris I. properties and characteristics of graphite. In: entegris I, editor. USA2013.

[21] Ltd ES. THE ELEMENT SIX CVD DIAMOND HANDBOOK Element Six Ltd: Element Six Ltd; 2015 [cited 2016]. Available from: http://e6cvd.com/media/wysiwyg/pdf/E6_CVD_Diamond_Handbook.pdf.

[22] Strekalov V. Lindeman's criterion: diamond graphitization temperature and its dependence on external pressure. arXiv preprint arXiv:12081535. 2012.

[23] Jungnickel G, Latham C, Heggie M, Frauenheim T. On the graphitization of diamond surfaces: the importance of twins. Diamond and Related Materials. 1996;5(1):102-7.

[24] Xu F, Hu H, Zuo D, Xu C, Qing Z, Wang M. Numerical analysis of Nd: YAG pulsed laser polishing CVD self-standing diamond film. Chinese Journal of Mechanical Engineering. 2013;26(1):121-7.

[25] Lutz G. Semiconductor radiation detectors: Springer; 1999.

[26] Koeck FA, Nemanich RJ. Low temperature onset for thermionic emitters based on nitrogen incorporated UNCD films. Diamond and Related Materials. 2009;18(2):232-4.

[27] MATHUR S. THE THERMIONIC WORK FUNCTION OF GRAPHITE——III. Proc Nat Acad Sci. 1952;19(2).

[28] Sze SM, Ng KK. Physics of semiconductor devices: John wiley & sons; 2006.

[29] Hamel L-A, Julien M. Generalized demonstration of Ramo's theorem with space charge and polarization effects. Nuclear Instruments and Methods in Physics Research Section A: Accelerators, Spectrometers, Detectors and Associated Equipment. 2008;597(2):207-11.

[30] Cornelius IM, Orlic I, Siegele R, Rosenfeld AB, Cohen DD. Ion beam induced charge collection time imaging of a silicon microdosimeter. Nuclear Instruments and Methods in Physics Research Section B: Beam Interactions with Materials and Atoms. 2003;210:191-5.

[31] Santin G. Normalisation modelling sources. Geant4Tutorial; Paris, France2007.

[32] Jarlskog CZ, Paganetti H. Physics settings for using the Geant4 toolkit in proton therapy. IEEE Transactions on Nuclear Science. 2008;55(3):1018-25.

[33] Chauvie S, Guatelli S, Ivanchenko V, Longo F, Mantero A, Mascialino B, et al. Geant4 low energy electromagnetic physics. Nuclear Science Symposium Conference Record, 2004 IEEE: IEEE; 2004. p. 1881-5.

[34] Prokopovich DA. Silicon on insulator microdosimetry for radiation protection in mixed radiation fields for aviation and space dosimetry: University of Wollongong; 2010.

[35] The quality factor in radiation protection: report of a joint task group of the ICRP and the ICRU to the ICRP and the ICRU. International Commission on Radiation Units and Measurements, 1986 Contract No.: 40.

[36] Kononenko T, Ralchenko V, Vlasov I, Garnov S, Konov V. Ablation of CVD diamond with nanosecond laser pulses of UV–IR range. Diamond and related materials. 1998;7(11):1623-7.

[37] Gabrysch M. Electronic properties of diamond: Institutionen för teknikvetenskaper; 2008.

[38] Majdi S. Electronic Characterization of CVD Diamond: UPPSALA University; 2010.

[39] Kellerer AM, Hahn K. Considerations on a revision of the quality factor. Radiation research. 1988;114(3):480-8.

[40] Chiriotti S, Moro D, Conte V, Großwendt B, Vanhavere F, Vynckier S. Indirect method to monitor the site size of sealed TEPCs. Radiation Measurements. 2016;85:26-31.